Summer 2021

Heterogeneous Extended Langmuir Model with a Truncated Multi-Normal Energy Distribution for Fitting Unary Data and Predicting Mixed-Gas Adsorption Equilibria

Sofia Tosso

Heterogeneous Extended Langmuir Model with a Truncated Multi-Normal Energy Distribution for Fitting Unary Data and Predicting Mixed-Gas Adsorption Equilibria

by

Sofia Tosso

Industrial Civil Engineering
Universidad Autónoma de Chile, 2017

Submitted in Partial Fulfillment of the Requirements

For the Degree of Master of Science in

Chemical Engineering

College of Engineering and Computing

University of South Carolina

2021

Accepted by:

James A. Ritter, Director of Thesis

Armin D. Ebner, Reader

John R. Monnier, Reader

Tracey L. Weldon, Interim Vice Provost and Dean of the Graduate School

ACKNOWLEDGMENTS

I would like to express my deepest gratitude to my advisor, Dr. James Ritter, for his support and advice throughout my master studies. I would like to thank Dr. Armin Ebner for guiding me and helping me with the questions that I brought him.

I also would like to express my dearest thanks to my Parents and my brothers and sister for their support to me.

My thanks also go to all the members that served in my master defense committee: Dr. Monnier, Dr. Ritter, and Dr. Ebner.

I would like to give thanks to the staff member such as the Charles Holland and Marjorie Nicholson for their very precious help. Also, I want to thank Behnam Fakhari to be part in my topic research.

Finally, I would like to thanks to all the friends that I made in the Master program in United State that support me this two year.

ABSTRACT

A heterogeneous extended Langmuir model (HEL) that uses a truncated frequency energy distribution based on a one, two or three normal distributions is presented to predict gas adsorption mixtures of single, binary, and ternary gas experimental data involving CO2, H2S and C3H8 on H-modernite reported in the work of Ritter et al (1986) in terms of both solid phase molar fractions and total loadings. These models were initially fitted against single gas data and then used to predict binary data and to establish the type of perfect correlations, whether positive or negative, exist amongst these three species. The models then used to predict the ternary data using the perfect correlations previously determined. A dual Langmuir process (DPL), the parameters of which were already determined elsewhere (Ritter et al., 2011) was also used against all experimental data for comparison. In general, the HEL models proved to be fundamentally correct mathematically and able to predict viable correlations among CO2, H2S and C3H8 on H-modernite, with CO2-H2S following a perfect positive correlation, CO2- C3H8 following a perfect negative correlation and H2S-C3H8 following a perfect negative correlation, which is consistent with the fact that both CO2 and H2S are polar gasses while C3H8 is nonpolar. The quality of the predictions among the HEL models were mixed and despite their complexity, none of them were able to match an apparent superior predictive ability of the DPL model, a result that was quite surprising because of the over simplicity of the latter. This reveals the strong ability of the DPL model to predict mixtures and that complex models such as the HEL presently discussed may not lead to better results.

TABLE OF CONTENTS

LIST OF TABLES

LIST OF FIGURES

INTRODUCTION

In order for models or correlations for mixed-gas adsorption to be crucial for the design of absorptive gas separation processes, they must be able to predict the equilibrium amount adsorbed (Yang, 1997). The problem with adsorption of multicomponent gas mixtures, compared to pure component adsorption, is that they are more demanding from a theorical and experimental point of view (Sanchez Varretti et al., 2016). Despite many studies in the last decades, there are some aspects of multicomponent adsorption that are not completely solved yet. One of such aspects is correctly tackling the fact that the adsorbents are energetically heterogeneous. Further, they do not only contain a distribution of adsorption sites but also the adsorbate-adsorbent interactions may be quite different for different adsorbates (Sircar, 1987). This must be taken into account when describing mixed-gas adsorption.

There are several models that have been developed as a deviation from the basic homogeneous Langmuir model to account for the surface energy heterogeneity of a surface. Toth, multisite, multiple process Langmuir are few examples of the most used analytical models to account for surface energetic heterogeneity. Other models rest on continuous energy distribution functions to account for the same (Hoory & Prausnitz, 1967; Sircar, 1984; Valenzuela et al., 1988), a concept that was originally proposed by Ross and Olivier in 1960 who stated that the heterogeneity of a solid surface must be reflected in the distribution of adsorptive potential energies that it offers to an adsorbate (Ross & Olivier,

1961). They proposed the well-known integral formula to express the adsorption isotherm of a pure gas in terms of this distribution. In 1975, Jaroniec and Rudzinski extended the integral formula to multi-gas adsorption (Rudziński & Jaroniec, 1974). The Unilan model was conceptually derived from this idea assuming a uniform surface distribution of energies. The problem remains however as to how these integral models be can extended to predict mix-isotherms.

There are not many papers that focus on the measurement of multi-gas adsorption isotherms (Jaroniec & Rudziński, 1975), and most of them do not go beyond binary gas mixtures. To solve this problem, Myers and Prausnitz (Myers & Prausnitz, 1965), developed the well-known ideal sorption solution (i.e., IAS) theory to predict mix isotherms directly from the isotherms of single gasses using on pure thermodynamic principles. However, the approach is mathematically intensive, and the results are not always accurate. Instead most modelling efforts are usually directed in predicting mix isotherm behavior from pure isotherms using modified extended forms of the isotherm models, whether from analytical or integral, to predict adsorption of pure gasses, models, to account for the adsorption of mixtures.

The problem that immediately arises from these extended models is that they do not directly establish, or it is left entirely to the modeler, as to how the adsorption surface energies for the individual gasses correlate or, in particular, they do not establish that gasses in the mixture perfectly correlate with others in positive of negative fashion (Jaroniec & Madey, 1988) The literature addressing this concern is rather scant. Valenzuela and Myers only explicitly indicated that they used perfect correlation when fitting their models to CO_2, H_2S and propane adsorption in binary and ternary mixtures (Valenzuela et al, 1988).

Ritter 2011 (Ritter et al., 2011) proposed an energetic site-matching approach to account for both perfect positive (PP) and perfect negative (PN) correlations in predicting binary and ternary mixtures using the dual process Langmuir (DPL) model. Their results show that some gases act in a perfect positive correlation, and others with a perfect negative correlation fashion and that those correlation are consistent with polar nature of the species, with very good predictions.

The objective of this thesis is to evaluate whether a more complex model could do a better job than the DPL model used by Ritter et al. (2011) to predict mix gas adsorption of binary and ternary data presented in the work of Talu and Zwiebel (1986). In this regard an integral model as proposed by Ross and Olivier (Ross & Olivier, 1961) that used one, two and three normal distribution for the adsorption energies using the extended Langmuir for local adsorption and with a proposed methodology similar to that used by Valenzuela et al. (1988) to include perfect negative in addition to perfect positive correlations between the species is evaluated.

CHAPTER 1

HETEROGENEOUS LANGMUIR MODEL WITH A TRUNCATED MULTI-NORMAL ENERGY DISTRIBUTION FOR FITTING UNARY DATA AND PREDICTING SINGLE-GAS ADSORPTION EQUILIBRIA

1.1 Introduction

The general methodology for studying surface energetic heterogeneity is to consider a pure gas isotherm applied locally to describe adsorption on a patch of surface and integrate it over an energy distribution (Ross and Olivier, 1964). So, the adsorption equilibria of a single-gas on an adsorbent is considered to be the minimum sources of information needed to define the interactions between the gas-solid pair (Sircar, 1987). There are many authors that applied this method to predict multi-component adsorption equilibria from the single-gas adsorption equilibria (Jaroniec & Rudziński, 1975; Valenzuela et al., 1988; Kapoor et al., 1990).

In this chapter, the integral model by Ross and Olivier (1961) is used to fit pure isotherms of CO_2, H_2S and propane based the work of Talu and Zwiebel (1986). The integral model uses the local Langmuir isotherm with an energy surface distribution described by either one, two or three truncated normal functions. All the results are compared with the dual process Langmuir model studied of Ritter paper (Ritter et al., 2011).

1.2 Mathematical Model

1.2.1 Multi-normal energy distribution for heterogeneous Langmuir model for single gas adsorption

The adsorption isotherm of a pure species i at a temperature T and pressure P on an adsorbent containing a surface characterized by a distribution of adsorptive patches of individual energies is given by (Ross & Olivier, 1961) :

$$\mathrm{n}_i(T,P) = \int_{\Delta} n_i(T,P,\varepsilon) f_i(\varepsilon) d\varepsilon \tag{1.1}$$

Where $n_i(T, P, \varepsilon)$ is the number of species i adsorbed on a homogeneous patch of energy ε (i.e., local adsorption isotherm); $f_i(\varepsilon)$ is the energy distribution that is unique to species i; and Δ represents the domain that encompasses all the possible values for adsorption energies in the adsorbent. The integral of $f_i(\varepsilon)$ must satisfy:

$$\int_{\Delta} f_i(\varepsilon) d\varepsilon = 1 \tag{1.2}$$

In the present work, $n_i(T, P, \varepsilon)$ and $f_i(\varepsilon)$ are respectively described by the Langmuir isotherm and the truncated multi-normal energy distribution function. The Langmuir isotherm is given by

$$n_i(T,P,\vec{y},\varepsilon) = \frac{n_{s,i} b_i(\varepsilon) P_i}{1 + b_i(\varepsilon) P_i} \tag{1.3}$$

where $n_{s,i}$, $b_i(\varepsilon)$ and P_i are saturation loading, the affinity, and the partial pressure of species i, respectively. $\mathrm{n}_{s,i}$ and $b_i(\varepsilon)$ are both temperature dependent and defined as

$$n_{s,i} = n_{so,i} + \frac{n_{sT,i}}{T} \tag{1.4}$$

$$b_i(\varepsilon) = b_{o,i} \exp\left(\frac{\varepsilon}{RT}\right) \tag{1.5}$$

Where $n_{so,i}$, $n_{sT,i}$, and $b_{o,i}$ are fitting parameters to be determined .The truncated multinormal distribution $f_i(\varepsilon)$ is defined as a sum of either one, two or three normal energy distributions,

$$f_i(\varepsilon) = \frac{\sum_k^{n_{ND}} f_{ND,i,k}(\varepsilon) * g_k}{1 - F_i(0)} \qquad n_{ND} = 1, 2 \text{ or } 3 \tag{1.6}$$

where the probability density function $f_{ND,j,k}(\varepsilon)$ is given by:

$$f_{ND,i,k}(\varepsilon) = \frac{1}{2}\frac{1}{\pi^{1/2}\sigma_{i,k}} \exp\left(-\frac{1}{2}\left(\frac{\varepsilon - \mu_{i,k}}{\sigma_{i,k}}\right)^2\right) \tag{1.7}$$

and where $F_i(\varepsilon)$ is the cumulative form of the energy distribution function that has been evaluated at $\varepsilon = 0$ to truncate the energy distribution from negative energies while satisfying Eq. 2). For the multinormal distribution,

$$F_i(\varepsilon) = \frac{1}{2}\sum_{k=1}^{n_{ND}} g_{i,k}\left(1 + erf\left(\frac{\varepsilon - \mu_{i,k}}{\sigma_{i,k}\sqrt{2\pi}}\right)\right) \qquad n_{ND} = 1, 2 \text{ or } 3 \tag{1.8}$$

$\sigma_{j,k}$ and $\mu_{j,k}$ are the fitting parameters corresponding to the standard deviation and the mean values of the energy. The $g_{i,k}$ parameters are also fitting parameters and correspond to weighing factors that satisfy

$$\sum_{k=1}^{n_{ND}} g_{i,k} = 1 \tag{1.9}$$

1.2.2 The Single-Gas Dual Process Langmuir Model

This model is a dual-process version of the Langmuir model for the predicting mixed gas adsorption equilibria (26). The single-gas DPL model describe the adsorption of a gas i on a heterogeneous adsorbent that is composed of two homogeneous but energetically different patched. Because it uses the Langmuir model, all the assumptions of that model apply in each patch, and both patches do not interact with each other (Langmuir). The amount adsorbed n_i, for component i is given by

$$n_i = \left(\frac{n_{1,i}^S b_{1,i} P}{1+b_{1,i}P}\right)_{site\ 1} + \left(\frac{n_{2,i}^S b_{2,i} P}{1+b_{2,i}P}\right)_{site\ 2} \quad (1.10)$$

where $n_{1,i}^S$ and $b_{1,i}$ are the saturation capacity and the affinity parameter on site 1, $n_{2,i}^S$ and $b_{2,I}$ are the parameters on site 2, and P is the absolute pressure. The affinity parameter for the two different sites can be defined with equation 5.

1.3 Results and discussion

To evaluate the quality of the Heterogeneous Extended Langmuir model (HEL), parameters of the single gas isotherms (Eqs. 1.1 through 1.8) were obtained first. For a gas species i, these parameters include $n_{so,i}$, $n_{sT,i}$, and $b_{o,i}$; together with $\mu_{i,1}$, and $\sigma_{i,1}$ with $g_{i,1} = 1$ if a single normal energy distribution is used; or together with $\mu_{i,1}$, $\sigma_{i,1}$, $\mu_{i,2}$, $\sigma_{i,2}$, and $g_{i,1}$ with $g_{i,2} = 1 - g_{i,1}$ if a dual normal energy distribution is used; or together with $\mu_{i,1}$, $\sigma_{i,1}$, $\mu_{i,2}$, $\sigma_{i,2}$, $\mu_{i,3}$, $\sigma_{i,3}$, $g_{i,1}$, and $g_{i,2}$ with $g_{i,3} = 1 - g_{i,2} - g_{i,1}$, if a triple normal energy distribution is used. In other words, a total of 5, 8 and 11 fitting parameters in case of using a single, dual, and triple normal energy distribution. A compensated sum of squared logarithm errors (CSSLE) shown below was minimized with the aid of Excel Solver to

determine these fitting parameters that produces the loadings from the isotherm model of pure species i $n_{model,i,k}$ (Eqs. 1.1 through 1.9) to best predict the experimental data $n_{exp,i,k}$:

$$CSSLE = \sum_{l=1}^{n_E} \left[\left[\ln \left(\frac{n_{i,model,l}}{n_{i,exp,l}} \right) \right]^2 \theta_{i,l} \right] \tag{1.11}$$

Where n_E is the number of experimental data and $\theta_{i,k}$ is compensating parameter that account for the uneven separation of the experimental pressures that is defined by:

$$\theta_{i,l} = \begin{cases} p_{i,exp,l} & l=1 \\ p_{i,exp,l} - p_{i,exp,l-1} & l>1 \end{cases} \tag{1.12}$$

In the case of DPL model, the parameters were extracted directly from (Ritter et al., 2011). In this model the author used the smallest sum of the squared error to minimize the relative differences between the predicted and the experimental amount adsorbed for all the different temperature

$$e = \frac{100}{N} \sum_{i=1}^{n_E} \left[\frac{n_p - n_e}{n_e} \right] \tag{1.13}$$

Where n_c and n_p are the predicted and experimental amounts adsorbed. In this model, every component will have six parameters and a corresponding average relative error (ARE). The ARE for the total amount adsorbed is defined as

$$ARE(\%) = \frac{100}{N} \sum_{i=1}^{n_E} \left[\frac{n_p - n_e}{n_e} \right] \tag{1.14}$$

In Appendix Table A.1, it is possible to see the parameters calculated in Ritters paper for CO_2, H_2S and propane in h-modernite (Ritter et al., 2011). The ARE es very low in 3 cases, being CO_2 the biggest value.

To test the model, pure, binary, and ternary experimental data involving CO_2, H_2S and C_3H_8 on H-modernite reported elsewhere (Talu & Zwiebel, 1986) was utilized. The values of the fitted parameters using any of the single, dual, or triple, normal energy distributions against pure gas experimental data of the above three gasses are given in Table 1, and the corresponding fitted curves are shown in Figure 1. For comparison, Table 1 also includes the CSSLE values using the dual process Langmuir (DPL) Model, the parameters of which were determined elsewhere (Ritter et al., 2011)against the same experimental data, with its corresponding curves shown in Fig. 1. The semi-log graph of the energy distribution function is used to see more clearly where the peaks of the normal distributions are. All experimental data is represented with symbols. In using Eq. 1.11, models were simultaneously fitted against the experimental data at all different temperatures available for a given species. To avoid very narrow normal distributions of the fits, the value of the standard deviations $\sigma_{i,k}$ were limited to be no less than 5 K.

The left-hand side panels of Fig. 1.1 show that all three HEL models fit relatively well the experimental data with the one using one normal distribution predicting distinctively more poorly than the other two, with the worse one being the one fitting the propane experimental results. The HEL model using three normal distribution showed the best fitting in all species but with CSSLE values only slightly better than those for the one using two normal distribution. The DPL model, in contrast, showed similar predicting behavior that the HEL models using two and three normal distributions for the case of H_2S and C_3H_8. The CSSLE values (Table 1.1) however for HEL models with two or three normal distributions displayed significantly better than the DPL model.

This is likely because the fitting parameters of the DPL model were determined by minimizing a sum of squared errors other than the CSSLE defined in Eq. 1.11. (Ritter et al., 2011). In contrast, for the case of CO_2 the DPL predicted the experimental data very poorly, principally because this model was originally fitted against a smaller set of experimental data at the higher loadings (i.e, > 0.8 mol/kg) (Ritter *et al.*, 2011), as it can be seen in Fig1a that at these loadings the DPL model predicts quite well the experimental data.

The right-hand side panels of Fig. 1.1 show the corresponding energy distributions for the three HEL models where the one, two and three normal distributions can be clearly observed. In a couple of instances, the HEL model required significant truncation as it was with the one with one normal distribution for CO_2, and the one with two normal distribution for H_2S. It is noteworthy that in some instances the fits involved very narrow distributions, with $\sigma_{i,k}$ values below 20 kPa. A particular peculiarity is the case of the HEL model with three normal distributions for H_2S, where each individual normal distribution presented $\sigma_{i,k}$ below 10 K, suggesting the existence of three patches with very distinct energies for this species on H-modernite.

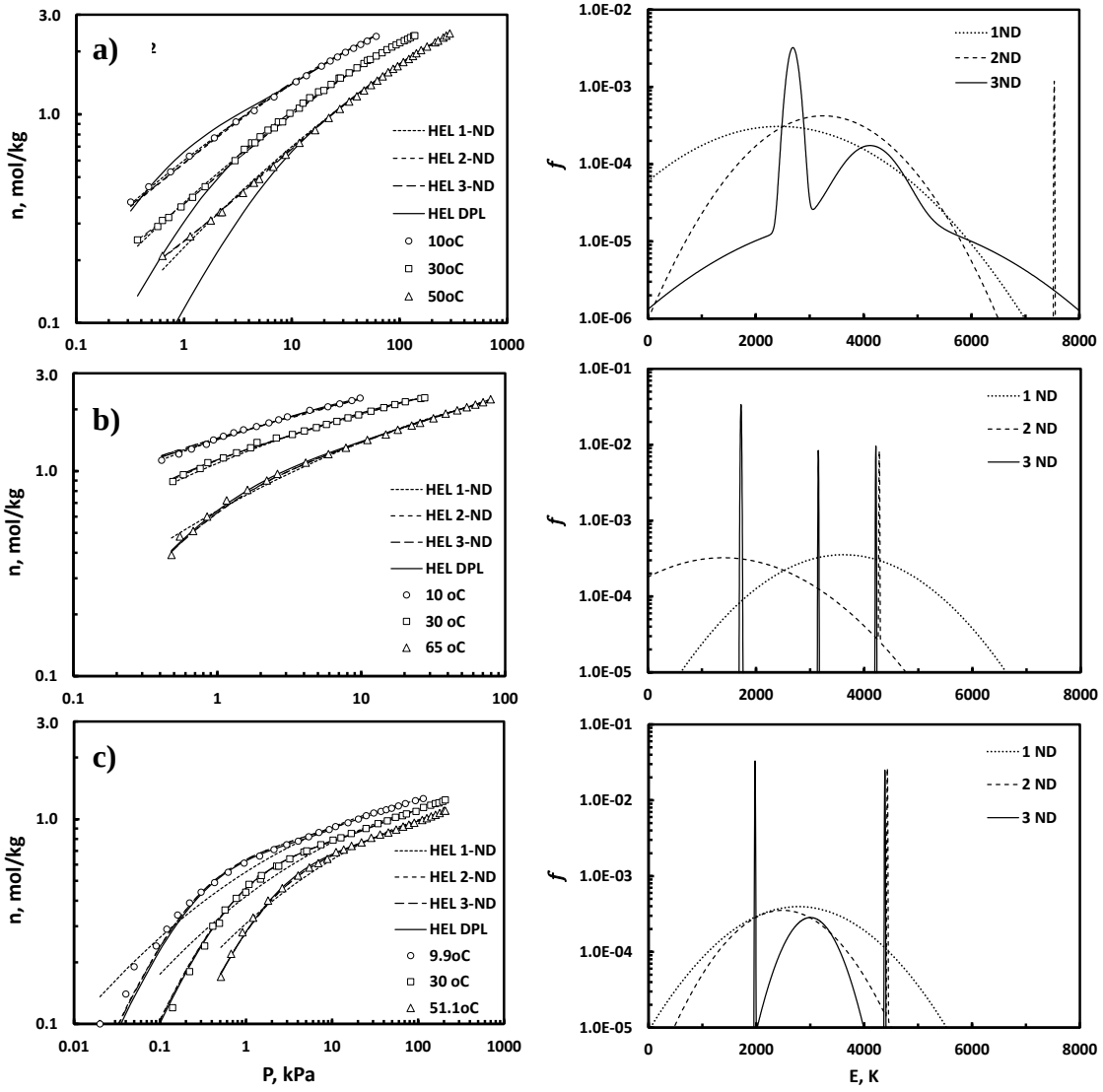

Figure 1.1 Fitted isotherms (left) and their corresponding energy distribution functions (right) for a) CO_2, b) H_2S and c) C_3H_8 for the HEL models using 1, 2 or 3 normal distributions and the DPL model against experimental results of these species on H-mordenite (Talu & Zwiebel, 1986)

Table 1.1 Fitting parameters and CSSLE values for the HEL model using one, two or three normal energy distributions against pure gas experimental isotherms for CO_2, H_2S and C_3H_8 on H-modernite that are shown in Fig. 1. The CSSLE values of the DPL model using parameters determined (Ritter et al., 2011) are also included.

	CO_2				H_2S				C_3H_8			
Parameters	1ND	2ND	3ND	DPL	1ND	2ND	3ND	DPL	1ND	2ND	3ND	DPL
σ_1, K	1345.65	5.00	1707.52	-	1125.63	1282.11	9.15	-	1012.77	755.24	5.00	-
μ_1, K	2434.17	7534.56	3984.87	-	3617.2	1390.79	1722.24	-	2781.94	2489.05	4384.21	-
g_1	1.0000	0.0150	0.0854	-	1.0000	0.9083	0.7730	-	1.0000	0.6683	0.3144	-
σ_2, K	-	933.07	93.36	-	-	5.00	5.00	-	-	5.00	5.00	-
μ_2, K	-	3252.59	2689.00	-	-	4278.79	3151.58	-	-	4431.11	1976.11	-
g_2	-	0.9850	0.7488	-	-	0.0917	0.1061	-	-	0.3317	0.4139	-
σ_3, K	-	-	430.36	-	-	-	5.00	-	-	-	381.99	-
μ_3, K	-	-	4120.97	-	-	-	4214.36	-	-	-	3003.22	-
g_3	-	-	0.1658	-	-	-	0.1208	-	-	-	0.2717	-
CSSLE	86.72	58.52	44.74	146.30	47.59	16.55	11.08	44.89	317.46	34.08	33.47	48.63

1.4 Conclusions

The heterogeneous single gas adsorption model, using a truncated multi-normal distribution, and extended Langmuir equation, has been formulated to calculate the parameters that are going to be used in mixture-gas adsorption. It was calculated to the cases of one, two and three normal distribution and DPL model for the gases CO_2, H_2S and propane. In the DPL model, the results were calculated directly from the experimental data of Ritters paper (Ritter et al., 2011). The results showed that in the case of HEL model improved with larger number of ND. In the case of 2-ND and 3-ND, they display similar fitting behavior. In H_2S and propane for 1-ND showed bad results compare with 2-ND and 3-ND.

In the DPL model, it is showed a similar although worse predicting behavior that the HEL models 2-ND and 3-ND for the case of H_2S and propane. This is because the DPL model was not fitted against the CSSLE as the objective function. They used the equation (1.13) like the objective function. For the case of CO_2, DPL showed bad predictions in the low-pressure region. That data was not including in Ritter et. al (2011). But this different is irrelevant because most of the conditions that are study in mix-isotherm do not involve low pressure of CO_2.

In the case of the energy distribution, it is possible to observe like in 3-ND H_2S very narrow peaks. That can mean the existence of energetically uniform superficial patches.

1.5 Nomenclature

b_i = affinity parameter of component *i*, kPa^{-1}

$b_{o,i}$ = pre-exponential factor of component *i*, kPa^{-1}

$b_{1,i}$ = pre-exponential factor of component *i* on site 1, kPa^{-1}

$b_{2,i}$ = pre-exponential factor of component *i* on site 2, kPa^{-1}

f_i = energy distribution function of component i

$f_{ND,i,k}$ = probability density function of 1, 2 or 3 normal distribution (ND), of species *i* and on-site *k* (1, 2, or 3)

F_i = cumulative energy distribution function of component i

$g_{i,k}$ = weight factor of component *i*, on site *k* (1, 2, or 3)

n_e = experimental amount adsorbed, mol/kg

n_E = number of experimental data

n_{ND} = number of normal distributions

n_i = amount adsorbed of component *i*, mol/kg

n_p = predicted amount adsorbed, mol/kg

n_T = total amount adsorbed, mol/kg

$n_{i,model,l}$ = predicted amount adsorbed from the model of component *i*, on site *l*, mol/kg

$n_{i,exp,l}$ = experimental amount adsorbed from the model of component *i*, on site *l*, mol/kg

$n_{s,i}$ = saturation capacity of component *i*, mol/kg

$n_{1,i}^{s}$= saturation capacity of component *i* on site 1, mol/kg

$n_{2,i}^{s}$= saturation capacity of component *i* on site 2, mol/kg

$n_{so,i}$ = constant term of saturation capacity of component *i*, mol/kg

$n_{sT,i}$ = temperature dependence term of saturation capacity of component *i*, mol kg^{-1} K^{-1}

P_i = partial pressure of species *i*, kPa

$p_{i,exp,l}$ = experimental pressure of species *i*, on site *l*, kPa

T = absolute temperature, K

Greek letters

Δ = Domain surface

ε_i = Energy of adsorption of component *i*, K

$\vartheta_{i,k}$ = compensating parameter that account for the uneven separation of the experimental pressure, of component *i*, site *k*, kPa

$\mu_{j,k}$ = mean value of species *j* on site *k* (1, 2, or 3), K

$\sigma_{j,k}$ = mean value of species *j* on site *k* (1, 2, or 3), K

CHAPTER 2

HETEROGENEOUS EXTENDED LANGMUIR MODEL WITH A TRUNCATED MULTI-NORMAL ENERGY DISTRIBUTION FOR FITTING UNARY DATA AND PREDICTING MULTI-GAS ADSORPTION EQUILIBRIA

2.1. Introduction

Numerous efforts have been made to develop techniques for prediction of multicomponent adsorption equilibria from the pure gas adsorption equilibrium of the components (Sircar, 1987). Valenzuela and Myers (1984) provide a good review of that theory. Their predictions in some cases showed acceptable predictions but unacceptable for others. So, it is necessary more work in that area. One of the problem could be that Valenzuela and Myers only explicitly indicated that they used perfect correlation when fitting their models to CO_2, H_2S and propane adsorption in binary and ternary mixtures (Valenzuela et al, 1988). Ritter 2011 (Ritter et al., 2011) proposed an energetic site-matching approach to account for both perfect positive (PP) and perfect negative (PN) correlations in predicting binary and ternary mixtures using the dual process Langmuir (DPL) model. Their results show that some gases act in a perfect positive correlation, and others with a perfect negative correlation, and that those correlation are consistent with polar nature of the species, with very good predictions.

In this chapter, the integral model by Ross and Olivier (1961) is used to predict binary and ternary mix isotherms of CO_2, H_2S and propane on H-mordenite based the work of Talu and Zwiebel (1986) using the fitted models obtained from single gas isotherms from the same work. The integral model for mixtures uses the extended local Langmuir isotherm with same energy surface distributions determined by the fitted single gas integral model and using a proposed methodology similar to that used by Valenzuela et al. (1988) to consider perfect negative in addition to perfect positive correlations between the species in the mixture. All the results are compared with the dual process Langmuir model studied of Ritter paper (Ritter et al., 2011).

2.2 Mathematical Model

2.2.1 Multi-Normal Energy Distribution in a Heterogeneous Extended Langmuir Model for multi-gas adsorption.

In the case of gas mixtures, the mixed adsorption isotherm of species i within a mixture of n_c components is

$$n_i(T,P,\vec{y}) = \int_{\vec{\Delta}} n_i(T,P,\vec{y},\vec{\varepsilon})\, f_i(\vec{\varepsilon}) d\varepsilon_1 d\varepsilon_2 .. d\varepsilon_{n_c} \qquad i = 1, 2,\ldots, n_c \quad (2.1)$$

where $\vec{y}$ and $\vec{\varepsilon}$ are vectors that simplify the representation of the values of the molar fractions y_1, y_2, etc, and corresponding energies ε_1, ε_2, etc, of all the species in the mixture. $n_i(T,P,\vec{y},\vec{\varepsilon})$ is the localized extended Langmuir (EL) Isotherm, i.e.,

$$n_i(T,P,\vec{y},\vec{\varepsilon}) = \frac{n_{s,i} b_i(\varepsilon_i) P_i}{1+\sum_{j=1}^{n_c} b_j(\varepsilon_j) P_j} \qquad i = 1, 2,.., n_c \quad (2.2)$$

with the $n_{s,i}$ and $b_i(\varepsilon)$ defined according to Eqs. 4) and 5). Because in each patch ε_1, ε_2, etc will be assumed to be perfectly correlated to each other, Eq. 11) becomes significantly simplified into the following expression

$$\mathrm{n}_i(T,P,\vec{y}) = \int_{\Delta} n_i\left(T,P,\vec{y},\varepsilon_i|\varepsilon_{ref}\right) f_{ref}\left(\varepsilon_{ref}\right) d\varepsilon_{ref} \quad \mathrm{i} = 1, 2,\ldots, \mathrm{n_c} \qquad (2.3)$$

where subscript ref stands for a species that is assumed to be as the referential species among the n_c species. The notation $\varepsilon_j|\varepsilon_{ref}$ is there to indicate that the energy ε_i of species i uniquely related (i.e., via perfect correlation) to a corresponding energy ε_{ref} of the referential species at any given patch. In this way, the energy distribution of the referential species, i.e., $f_{ref}\left(\varepsilon_{ref}\right)$, is used instead of $f_i(\varepsilon_i)$ in Eq. (12).

The unique relation between ε_i and the energy of the referential species ε_{ref} will depend on the type of correlation that exists between the two. Similar to what Valenzuela et al. (1988) proposed, if species i follows a perfect positive correlation with the referential species

$$F_{ref}^T\left(\varepsilon_{ref}\right) - F_i^T(\varepsilon_i) = 0 \qquad (2.4)$$

However, if species i follows a perfect negative correlation with the referential species

$$F_{ref}^T\left(\varepsilon_{ref}\right) + F_i^T(\varepsilon_i) = 1 \qquad (2.5)$$

where $F_{ref}^T\left(\varepsilon_{ref}\right)$ or $F_i^T(\varepsilon_i)$, correspond to the truncated form of the cumulative form of the energy distribution of the species i or the referential one, i.e.,

$$F_i^T(\varepsilon_i) = \frac{F_i(0) - F_i(0)}{1 - F_i(0)} \qquad \mathrm{i} = 1, 2,\ldots, \mathrm{n_c} \qquad (2.6)$$

A perfect positive (PP) correlation between two species as reflected by Eq. (2.4) assumes that the ordering of the sites from low to high energy values is the same for both species, while a perfect negative (PN) correlation between two species as reflected by Eq. (2.5) assumes that the ordering of the sites from low to high energy values for one species is reversed for the other species. Also, Eqs. (2.4) and (2.5) only express correlations between a given species and the reference one, but they lead to viability (Ritter *et al.*, 2011) when it comes to establishing correlations between two species other than the referential one. In other words, the way two non-referential species correlate with each other must be consistent with the way both correlate with the referential species.

2.2.2 Dual Process Langmuir for Binary Adsorption

In this model there are two sites where each component adsorbs on. So, there will be four different adsorbate-adsorbent free energies exist, two free energies for site A, and two free energies for site B. like in the HEL, this model can follow a PP or PN correlation. When component A sees site 1 as a high-free-energy site, and component B site 2 as the low-free-energy site there is a PP correlation with the adsorbate-adsorbent free energies. The amount adsorbed amount on binary mixture for each component is given by

$$n_{A,m} = \left(\frac{n^S_{1,A} P y_A b_{1,A}}{1+P y_A b_{1,A}+P y_B b_{1,B}}\right)_{site\ 1} + \left(\frac{n^S_{2,A} P y_A b_{2,A}}{1+P y_A b_{2,A}+P y_B b_{2,B}}\right)_{site\ 2} \tag{2.7}$$

$$n_{B,m} = \left(\frac{n^S_{1,B} P y_B b_{1,B}}{1+P y_A b_{1,A}+P y_B b_{1,B}}\right)_{site\ 1} + \left(\frac{n^S_{2,B} P y_B b_{2,B}}{1+P y_A b_{2,A}+P y_B b_{2,B}}\right)_{site\ 2} \tag{2.8}$$

On the other hand, when component A sees site 1 as a low-free-energy site, and component B site 2 as the high-free-energy site there is a PN correlation with the adsorbate-

adsorbent free energies. The amount adsorbed amount on binary mixture for each component is given by

$$n_{A,m} = \left(\frac{n_{1,A}^{S} P y_A b_{1,A}}{1+P y_A b_{1,A}+P y_B b_{2,B}}\right)_{site\ 1} + \left(\frac{n_{2,A}^{S} P y_A b_{2,A}}{1+P y_A b_{2,A}+P y_B b_{1,B}}\right)_{site\ 2} \quad (2.9)$$

$$n_{B,m} = \left(\frac{n_{1,B}^{S} P y_B b_{1,B}}{1+P y_A b_{2,A}+P y_B b_{1,B}}\right)_{site\ 1} + \left(\frac{n_{2,B}^{S} P y_B b_{2,B}}{1+P y_A b_{1,A}+P y_B b_{2,B}}\right)_{site\ 2} \quad (2.10)$$

where y_a and y_b are the gas-phase mole fraction of the components a and b. The total amount adsorbed is the summation of adsorbed amount of both components.

2.2.3 Dual Process Langmuir for Ternary Adsorption

The DPL model for binary considered that the designation of a site can have high or low free energy. If the components see this site in the same way is PP, and PN in the opposite way. But in ternary is necessary to include other affinity parameter. To simplify all the correlations, in Ritter's paper (Ritter et al., 2011) was applied some rules. In the case of PP, considering three components A, B and C, if A-B correlates PP, and B-C correlates PP, so A-C must correlate PP. So, the calculation of the adsorbent amounts of each component are

$$n_{A,m} = \left(\frac{n_{1,A}^{S} P y_A b_{1,A}}{1+P y_A b_{1,A}+P y_B b_{1,B}+P y_C b_{1,C}}\right)_{site\ 1} + \left(\frac{n_{2,A}^{S} P y_A b_{2,A}}{1+P y_A b_{2,A}+P y_B b_{2,B}+P y_C b_{2,C}}\right)_{site\ 2} \quad (2.11)$$

$$n_{B,m} = \left(\frac{n_{1,B}^{S} P y_B b_{1,B}}{1+P y_A b_{1,A}+P y_B b_{1,B}+P y_C b_{1,C}}\right)_{site\ 1} + \left(\frac{n_{2,B}^{S} P y_B b_{2,B}}{1+P y_A b_{2,A}+P y_B b_{2,B}+P y_C b_{2,C}}\right)_{site\ 2} \quad (2.12)$$

$$n_{C,m} = \left(\frac{n_{1,C}^{S} P y_C b_{1,C}}{1+P y_A b_{1,A}+P y_B b_{1,B}+P y_C b_{1,C}}\right)_{site\ 1} + \left(\frac{n_{2,C}^{S} P y_C b_{2,C}}{1+P y_A b_{2,A}+P y_B b_{2,B}+P y_C b_{2,C}}\right)_{site\ 2} \quad (2.13)$$

In the case of PN, considering three components A, B and C, if A-B correlates PN, and B-C correlates PN, so A-C must correlate PP. So, the calculation of the adsorbent amounts of each component are

$$n_{A,m} = \left(\frac{n^S_{1,A} P y_A b_{1,A}}{1+Py_A b_{1,A}+Py_B b_{2,B}+Py_C b_{1,C}}\right)_{site\ 1} + \left(\frac{n^S_{2,A} P y_A b_{2,A}}{1+Py_A b_{2,A}+Py_B b_{1,B}+Py_C b_{2,C}}\right)_{site\ 2} \quad (2.14)$$

$$n_{B,m} = \left(\frac{n^S_{1,B} P y_B b_{1,B}}{1+Py_A b_{2,A}+Py_B b_{1,B}+Py_C b_{2,C}}\right)_{site\ 1} + \left(\frac{n^S_{2,B} P y_B b_{2,B}}{1+Py_A b_{1,A}+Py_B b_{2,B}+Py_C b_{1,C}}\right)_{site\ 2} \quad (2.15)$$

$$n_{C,m} = \left(\frac{n^S_{1,C} P y_C b_{1,C}}{1+Py_A b_{1,A}+Py_B b_{2,B}+Py_C b_{1,C}}\right)_{site\ 1} + \left(\frac{n^S_{2,C} P y_C b_{2,C}}{1+Py_A b_{2,A}+Py_B b_{1,B}+Py_C b_{2,C}}\right)_{site\ 2} \quad (2.16)$$

These correlations see if the models are viable according to Ritter *et al.*, 2011 . In Appendix Table B.1 are the viable and nonviable PP and PN correlations for a ternary system where the model C-1 and C-5 was applied in those formulas.

2.3 Results and Discussion

2.3.1 Binary Mixture

Once single gas isotherm parameters are determined and the quality of their fits are established, the next step is to directly use them in equations (2.2) through (2.6) to predict mixed gas isotherms by assuming perfect positive or a perfect negative correlation among the species while maintaining consistency with the principle of viability (Ritter *et al.*, 2011) . To evaluate the quality of the predictions against experimental binary and ternary equilibrium data, the following expressions were used

$$\text{SSEn} = \sum_{l=1}^{n_E}\left[n_{T,model,l} - n_{T,exp,l}\right]^2 \quad (2.17)$$

$$\text{SSEx} = \sum_{l=1}^{n_E}\sum_{j=1}^{n_c-1}\left[x_{j,model,l} - x_{j,exp,l}\right]^2 \quad (2.18)$$

where the SSEn, and SSEx respectively are the sum of the squared errors of the total adsorption loadings and of the solid phase molar fractions. The total adsorption loadings and the solid phase molar fractions are respectively given by

$$n_T = \sum_{j=1}^{n_c} n_j \tag{2.19}$$

$$x_i = \frac{n_i}{\sum_{j=1}^{n_c} n_j} \tag{2.20}$$

Note that SSEx only carries out the sum of errors of nc-1 species to involve independent data only. Figs. *2.1* and *2.2* show the predictions of the different HEL models and the DPL model against experimental binary data involving CO_2, H_2S and C_3H_8 (Talu et al, 1986) at constant pressure and constant composition, respectively at 30 ^oC for both a perfect positive correlation and perfect negative correlation. CO_2 was used as the referential gas. The x and y values used in these panels correspond to those of CO_2 for the CO_2-H_2S and the CO_2-C_3H_8 pairs and to that of H_2S for the H_2S-C_3H_8 pair. The respective SSEx and SSEn values for the predictions in these figures are given in Tables *2.1* and *2.2*.

For the particular case of n_T-x plots for Fig. 2, where both variables involved in the graph are predicted (i.e., n_T and x_i) the SSEn values were not evaluated using the $n_{T,model}$ values predicted directly from the corresponding yi values. Instead, they used n_T values evaluated by linear interpolation using the closest two predicted $n_{T,model}$ $x_{i,model}$ pairs at the experimental $x_{i,exp}$. The x-y plots of Figure 2.1 also include the diagonal to display the possible predicted existence of azeotropes.

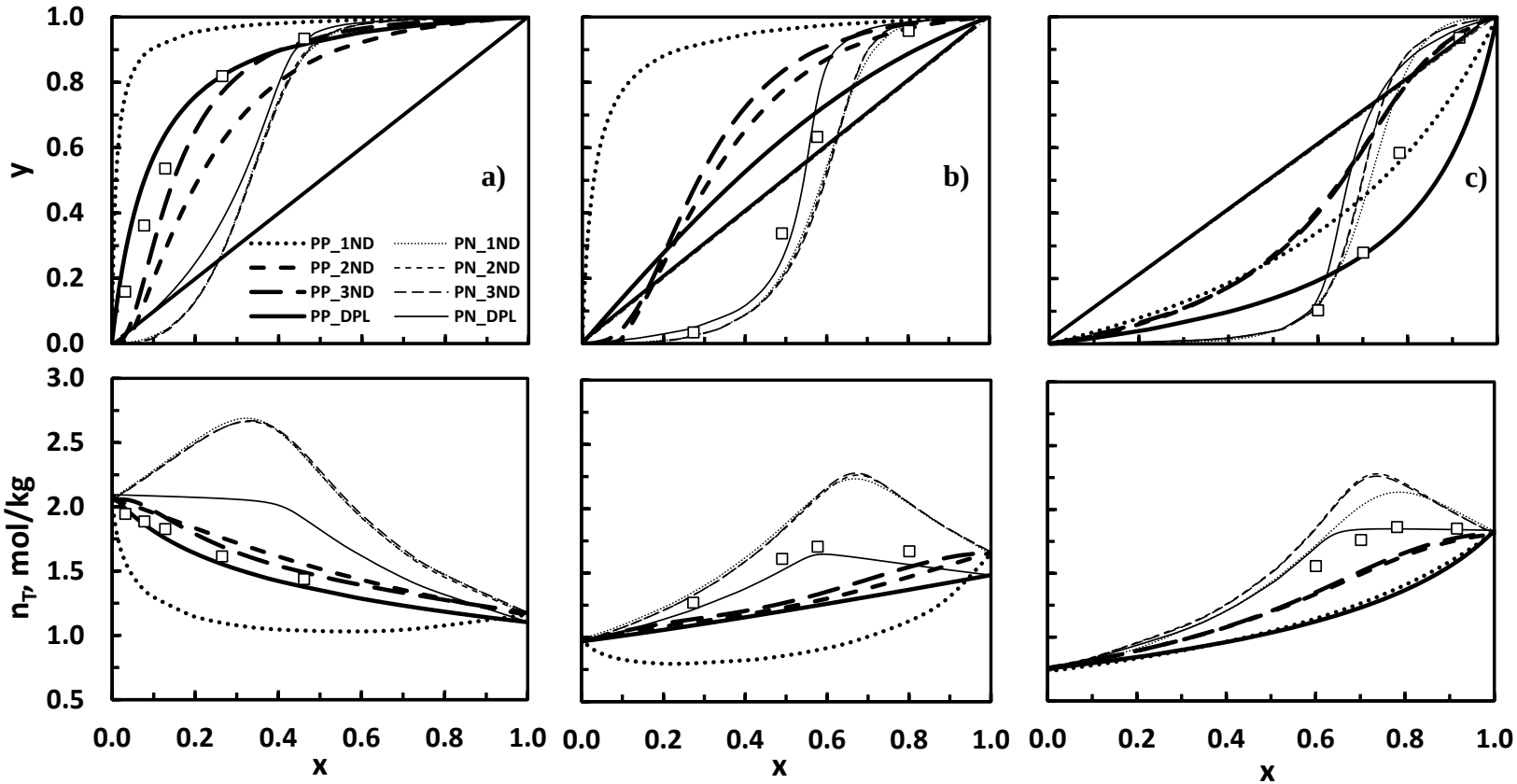

Figure 2.1 Predicted gas phase molar fractions (top) and total loadings (bottom) at given solid phase molar fractions from different models for a) CO_2- H_2S binary mixtures at 15 kPa and 30 ^oC b) CO_2-C_3H_8 binary mixtures at 40.9 kPa and 30 ^oC and c) H_2S-C_3H_8 binary mixtures at 8 kPa and 30 ^oC. Thick curves correspond to models using perfect positive correlations. Thin curves correspond to models using perfect negative correlations. Predictions of the DPL model are also included. The x and y values correspond to those of CO_2 in a) and b) and to that of H_2S in c)

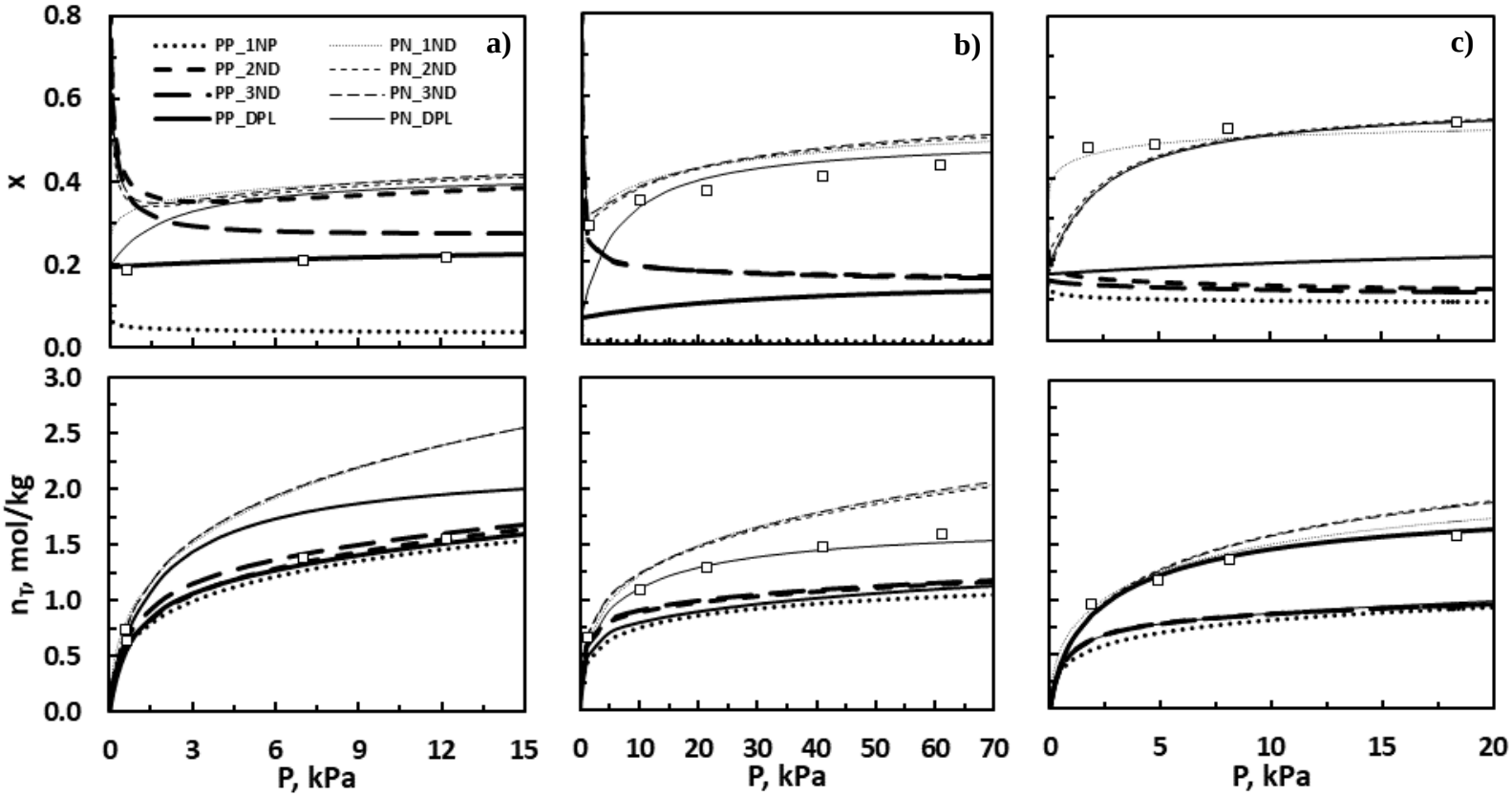

Figure 2.2 Predicted solid phase molar fractions (top) and total loadings (bottom) at given pressure from different models for a) CO_2-H_2S binary mixtures with y_{CO2} = 0.78 and 30 ^oC b) CO_2-C_3H_8 binary mixtures with y_{CO2} = 0.17 and 30 ^oC and c) H_2S-C_3H_8 binary mixtures with y_{H2S} = 0.0367 and 30 ^oC. Thick curves correspond to models using perfect positive correlations. Thin curves correspond to models using perfect negative correlations. Predictions of the DPL model are also included. The x values correspond to those of CO_2 in a) and b) and to that of H_2S in c)

Table 2.1 SSEx and SSEn values for the HEL model using 1, 2 or 3 normal energy distributions against experimental binary gas data for CO_2, H_2S and C_3H_8 on H-mordenite and for the pressure and temperature conditions shown in Fig. 2.1. The SSEx and SSEn values for the DPL model using parameters determined elsewhere (Ritter et al., 2011) are also included. Since the nT, and the xi values in Fig. 2.1 were all predicted at the given values of yi, the SSEn were evaluated using linearly interpolated values of nT,model,i from the two closest predicted nT,model Xi,model pairs at the experimental value of Xi,exp. The xi values used in these linear interpolations corresponded to those of CO_2 for the CO_2-H_2S and the CO_2-C3H_8 pairs and to that of H_2S for the H_2S-C_3H_8 pair.

Constant P									
		SSEx				SSEn*			
Gases	Correlation	1 ND	2 ND	3 ND	DPL	1 ND	2 ND	3 ND	DPL
CO_2-H_2S	PP	0.793	0.188	0.059	0.044	1.163	0.059	0.044	0.016
	PN	0.684	0.687	0.695	0.450	2.399	2.333	2.355	0.549
CO_2-C_3H_8	PP	1.270	0.379	0.502	0.207	1.729	0.386	0.288	0.495
	PN	0.048	0.057	0.064	0.020	0.361	0.332	0.349	0.025
H_2S-C_3H_8	PP	0.107	0.229	0.222	0.154	0.689	0.191	0.160	0.806
	PN	0.065	0.127	0.129	0.209	0.189	0.470	0.436	0.028

*Linearly Interpolated at the $X_{i,exp}$ values.

Table 2.2 SSEx and SSEn values for the HEL model using one, two or three normal energy distributions against experimental binary gas data for CO_2, H_2S and C_3H_8 on H-mordenite and for the gas composition and temperature conditions shown in Fig. 2.2. The SSEx and SSEn values for the DPL model using parameters determined elsewhere (Ritter et al., 2011) are also included.

		Constant y							
		SSEx				SSEn			
Gases	Correlation	1 ND	2 ND	3 ND	DPL	1 ND	2 ND	3 ND	DPL
CO_2-H_2S	PP	0.098	0.145	0.080	0.0002	0.055	0.037	0.014	0.049
	PN	0.107	0.124	0.138	0.063	1.160	1.182	1.181	0.349
CO_2-C_3H_8	PP	0.675	0.197	0.199	0.366	0.931	0.523	0.457	0.711
	PN	0.012	0.011	0.014	0.025	0.311	0.280	0.320	0.020
H_2S-C_3H_8	PP	0.652	0.532	0.567	0.408	1.178	0.912	0.944	0.931
	PN	0.001	0.015	0.018	0.018	0.030	0.115	0.112	0.017

In general, all models agree (based on the quality of the fits via eye inspection in Figs *2.1* and *2.2* and the corresponding SSEx and SSEn values in Tables *2.1* and *2.2* that the CO_2-H_2S follow a perfect positive correlation, that CO_2-C_3H_8 follow a perfect negative correlation and that H_2S-C_3H_8 follow a perfect negative correlation, in consistence with the viability principle (Ritter et al., 2011) and the fact that both CO_2 and H_2S are polar gasses while C_3H_8 is nonpolar. It is noteworthy that the predictions for the H_2S-C_3H_8 have assumed, for the case of perfect positive correlation, that In the Figures both H_2S and C_3H_8 were assumed to be perfectly correlated with CO_2, as the latter is the referential gas when using equation 12. However, identical predictions are obtained (results not shown) from same Eq. (2.3) if both H_2S and C_3H_8 are assumed negatively correlated with CO_2 instead. Similarly, for the case of perfect negative correlation, H_2S and C_3H_8 were respectively

assumed to be perfectly positively correlated and perfectly negatively correlated with CO_2 when using Eq. (2.3). And again, identical results are obtained if H_2S and C_3H_8 (results not shown) were respectively and conversely assumed to be perfectly negatively correlated and perfectly positively correlated with CO_2, instead. These identical predictions prove that the HEL model presently used is fundamentally correct and consistent with the viability principle (Ritter et al., 2011). It is also important to say that the SSEn numbers for the perfect negative correlation were about the same (Fig 2.1b bottom) and even worse (Fig. 2.2b) than those for the perfect positive correlation, the shape of the curves for the perfect negative correlation in both y-x and n_T-x plots in both Figs 2.1b and 2.1c were more qualitatively consistent with the shape of the experimental data.

In terms of the quality of the predictions there is no consistent trend as to which HEL model predicts the best in all results. In general, for the CO_2-H_2S pair (Figures 2.1a and 2.2a), the HEL model with three normal distributions and perfect positive correlation predicts the best. For the CO_2-C_3H_8 pair (Figures 2.1b and 2.2b), all HEL models under perfect negative correlation predict about the same. For the H_2S-C_3H_8 pair (Figures 2.1c and 2.2c), the HEL model with one normal distribution and perfect positive correlation predicts the best. Quite surprisingly, the DPL model generally showed to have a better predictive behavior than the HEL models. In fact, in several cases, prediction of the DPL model was even significantly better than the HEL models, as it was the case when predicting total loadings for the CO_2-C_3H_8 and the H_2S-C_3H_8 pairs. This strongly speaks of the goodness of the DPL model, which is attractive due to its simplicity compared to the relatively complex HEL models.

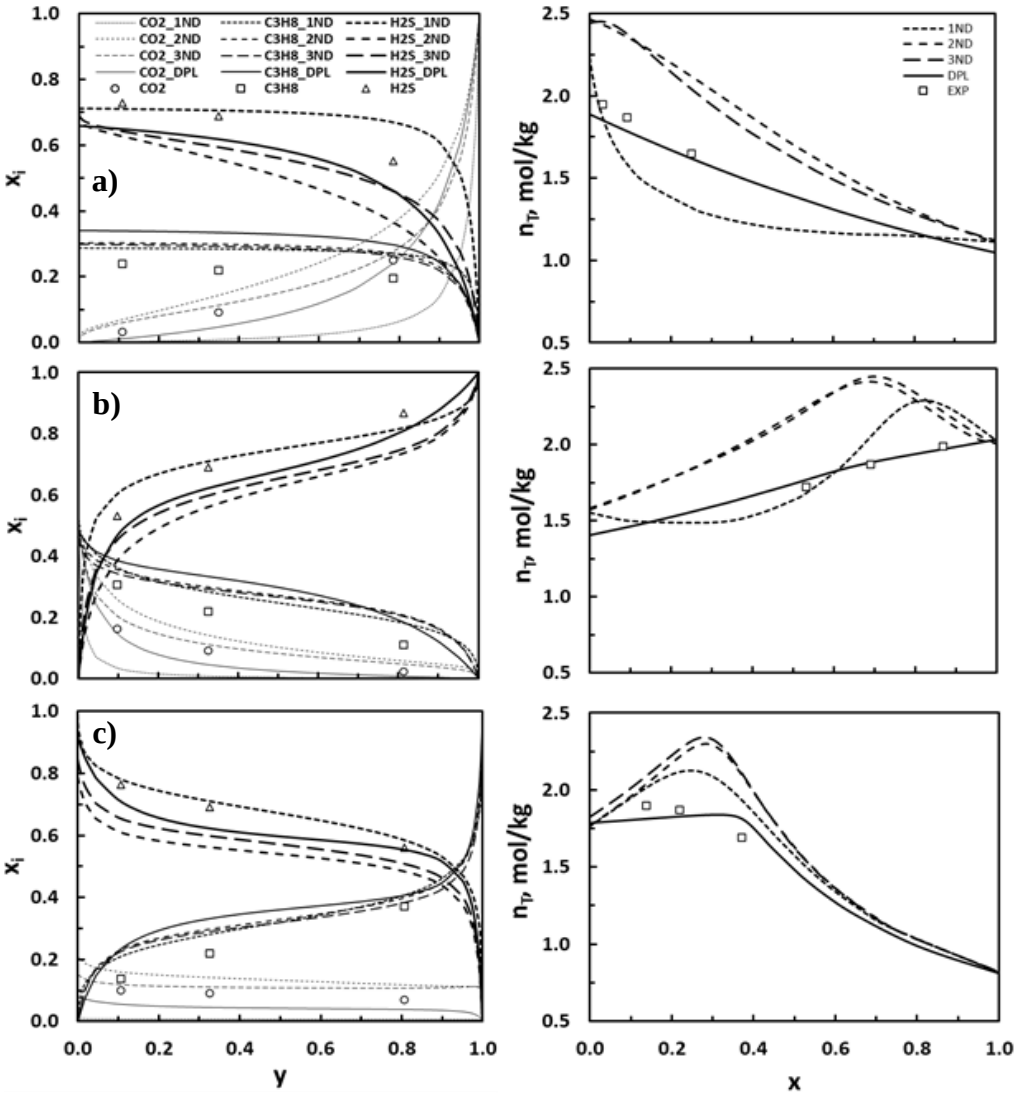

Figure 2.3 Predicted solid phase ternary molar fractions (left) and total loadings (right) for a) CO_2 b) H_2S and c) C_3H_8 paths at 13.35 kPa and 30 ^oC, with the y and x values in the x-axes corresponding to those of CO_2, H_2S and C_3H_8, respectively. In the CO_2 path, the gas molar ratio between C_3H_8 and H_2S is 1.0621. In the H_2S path, the gas molar ratio between C_3H_8 and CO_2 is 0.9635. In the C_3H_8 path, the gas molar ratio between CO_2 and H_2S is 1.0630.

2.3.2 Ternary Mixture

Figures 2.3 and 2.4 display the predictions of all HEL models as well as the BPL model for the ternary results for CO_2, H_2S and C_3H_8 on H-mordenite (Talu & Zwiebel, 1986) at 30^oC. The panels on the left-hand side show model predictions and experiments for the gas solid phase molar compositions while panels of the right-hand side show model predictions and experiments for the total loading. Figure 2.3 displays the results at constant pressure following what they described as the CO_2, H_2S and C_3H_8 paths. In these, the molar fraction of the species indicated in the path is varied while the ratio of the molar fractions of the other two species is maintained constant. Figure 5 displays the results at constant gas phase composition with varying pressures. It has assumed in the predictions of all models that H_2S and C_3H_8 follow a perfect positive correlation and a perfect negative correlation with respect to CO_2 which is consistent with the findings shown in Figs. 2.1 and 2.2. H_2S and C_3H_8, hence correlate perfectly negative with each other in these predictions. The corresponding SSEx and SSEn values for Figs 2.3 and 2.4 are shown in Table 2.3.

The figures as well as the SSEx and SSEn values show that the predictions of the HEL models are in general of limited quality at best only qualitatively following the trends of the solid phase more composition while missing both in shape and value the experimental results for the total loadings. Further the relative prediction quality of the different HEL models is mixed. For the solid molar composition results and based on the SSEx values of Table 2.3, the HEL model with two normal distributions showed to be best for the results following the CO_2 path, while the HEL model with three normal distributions showed to be best for the results following the H_2S and C_3H_8 paths at the constant

composition one. The HEL model with one normal distribution showed the worst prediction behavior but only an apparently ability to uniquely predict the solid molar fraction of H_2S best as it can be seen in Figs 2.3 and 2.4. In contrast the DPL model displayed a significantly stronger predicting ability over any of the HEL models, particularly when predicting the total loadings, being able to capture quite well both the values and the trends of the total loadings. This was equally reflected by the much lower SSEn (Table 2.3) values of the DPL model over the HEL models. In terms of predicting the solid molar compositions, the SSEx values in Table 2.3 showed that DPL model was relatively only equally as good but not best relative to the HEL models in any of the paths and in the constant composition results.

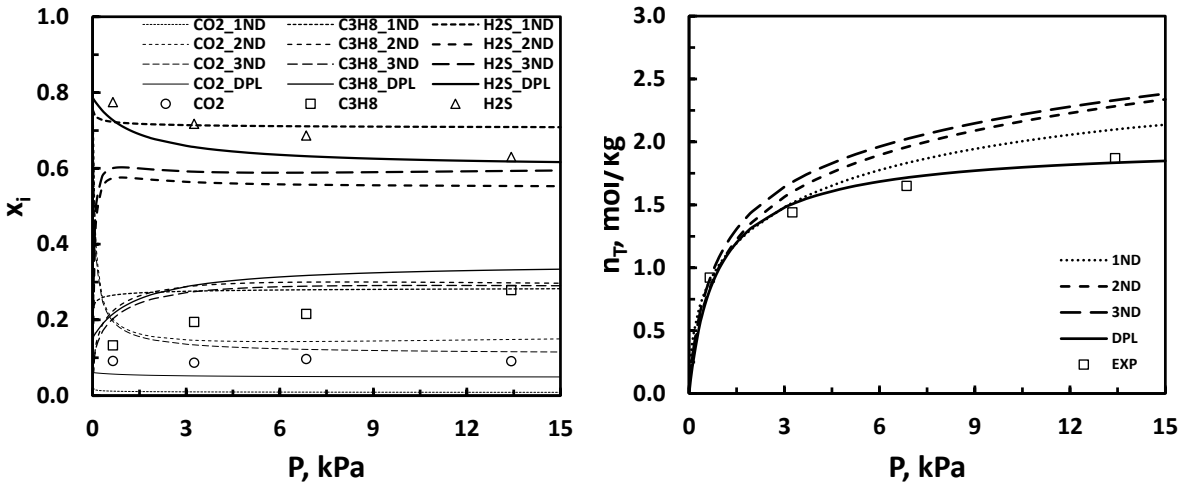

Figure 2.4 Predicted solid phase ternary molar fractions (left) and total loadings (right) for a fixed gas phase composition of CO_2, H_2S and C_3H_8 of 0.37, 0.31, and 0.32 respectively at a temperature of 30 ^oC.

Table 2.3. SSEx and SSEn values for the HEL model using one, two or three normal energy distributions against experimental ternary gas data for CO_2, H_2S and C_3H_8 on H-mordenite following either different concentrations paths for a fixed pressure and temperature or different pressures for a fixed gas phase composition and temperature as shown in Figs. 2.3 and 2.4. The SSEx and SSEn values for the DPL model using parameters determined elsewhere (Ritter et al., 2011) are also included. Since the n_T, and the x_i values in Fig. 2.3 were all predicted at the given values of yi, the SSEn were evaluated using linearly interpolated values of $n_{T,model,i}$ from the two closest predicted $n_{T,model}$ $X_{i,model}$ pairs at the experimental value of $X_{i,exp}$. The xi's used in these linear interpolations corresponded to those of CO_2, H_2S, and C_3H_8, for the CO_2 H_2S, and C_3H_8 paths, respectively.

	SSEx				SSEn			
	1 NED	2 NED	3 NED	DPL	1 NED	2 NED	3 NED	DPL
CO_2 Path	0.057	0.033	0.054	0.036	0.193	0.691	0.663	0.144
H_2S Path	0.036	0.031	0.018	0.027	0.109	0.607	0.639	0.003
C_3H_8 Path	0.030	0.024	0.015	0.028	0.132	0.303	0.373	0.025
Constant y	0.055	0.046	0.031	0.036	0.092	0.299	0.410	0.023

*Linearly Interpolated at the $X_{i,exp}$ values.

2.4 Conclusions

The quality of a Heterogeneous Extended Langmuir model (HEL) that uses truncated frequency energy distributions based on a one, two or three normal distributions was evaluated against single, binary and ternary gas experimental data involving CO_2, H_2S and C_3H_8 on H-mordenite in terms of both solid phase molar fractions and total loadings that were reported in the work of Talu and Zwiebel (Talu & Zwiebel, 1986) . These models were initially fitted against single gas data and then used to predict binary data and established the type of perfect correlations, whether positive or negative, exist amongst these three species and whether these correlations are consistent with the viability principle. Once such correlations were such correlations were established, the models used them to predict the above indicated ternary data. A dual Langmuir process (DPL), the parameters of which were already determined elsewhere (Ritter et al., 2011) was also used against all experimental data for comparison. In general, the HEL models proved to be fundamentally correct mathematically and able to predict viable correlations among CO_2, H_2S and C_3H_8 on H-mordenite, with CO_2-H_2S following a perfect positive correlation, CO_2-C_3H_8 following a perfect negative correlation and H_2S-C_3H_8 following a perfect negative correlation, which is consistent with the fact that both CO_2 and H_2S are polar gasses while C_3H_8 is nonpolar. The quality of the predictions among the HEL models were mixed. Sometimes using one normal distribution predicted the best results amongst all the three, in other results using either two or three normal distributions produced the best predictions. However, and despite their complexity, none of the HEL models were able to match an apparent superior quality of the DPL model to predict the above said binary and ternary experimental data, especially when predicting the total loadings of mixtures, wherein the

DPL were not only able to follow far better trends and intensities. This reveals the strong ability of the DPL model to predict mixtures, despite its simplicity to describe the heterogeneity of adsorbents in discrete two patch fashion. It also reveals that complex models that describe the heterogeneity of adsorbents in the form of complex energy distributions such as the ones used here may not lead to better results.

2.5 Nomenclature

b_i = affinity parameter of component *i*, kPa^{-1}

f_i = energy distribution function of component i

F_i = cumulative energy distribution function of component i

F_i^T = truncate cumulative energy distribution function of component i

n_c = number of components

n_E = number of experimental data

n_{ND} = number of normal distributions

n_i = amount adsorbed of component *i*, mol/kg

$n_{i,m}$ = amount adsorbed of component *i (=A,B, or C)* in the mixture, mol/kg

$n_{j,i}^s$= saturation capacity of component *i (=A,B, or C)* on site *j (= 1 or 2)*, mol/kg

n_T = total amount adsorbed, mol/kg

$n_{T,model,l}$ = total predicted amount adsorbed from the model, on site *l*, mol/kg

$n_{T,exp,l}$ = total experimental amount adsorbed from the model, on site *l*, mol/kg

$n_{s,i}$ = saturation capacity of component *i*, mol/kg

P_i = partial pressure of species *i*, kPa

P_i = absolute pressure, kPa

T = absolute temperature, K

x_i = adsorbed-phase mole fraction of component *i*

$x_{i,model,l}$ = predicted adsorbed-phase mole fraction from the model of component *i*, on site *l*

$x_{i,exp,l}$ = experimental adsorbed-phase mole fraction from the model of component *i*, on site *l*

y_i = gas-phase mole fraction of component *i*

Greek letters

Δ = Domain surface

ε_i = Energy of adsorption of component *i*, K

ε_{ref} = Energy of adsorption of the referential species, K

REFERENCES

Hoory, S. E., & Prausnitz, J. M. (1967). Monolayer adsorption of gas mixtures on homogeneous and heterogeneous solids. *Chemical Engineering Science*, *22*(7), 1025–1033. https://doi.org/https://doi.org/10.1016/0009-2509(67)80166-0

Jaroniec, M., & Madey, R. (1988). *Physical Adsorption on Heterogeneous Solids*. Elsevier. https://books.google.com/books?id=PGAUtAEACAAJ

Jaroniec, M., & Rudziński, W. (1975). Adsorption of gas mixtures on heterogeneous surfaces: The integral representation for a monolayer total adsorption isotherm. *Surface Science*, *52*(3), 641–652. https://doi.org/https://doi.org/10.1016/0039-6028(75)90093-X

Kapoor, A., Ritter, J. A., & Yang, R. T. (1990). An extended Langmuir model for adsorption of gas mixtures on heterogeneous surfaces. *Langmuir*, *6*(3), 660–664. https://doi.org/10.1021/la00093a022

Myers, A. L., & Prausnitz, J. M. (1965). Thermodynamics of mixed-gas adsorption. *AIChE Journal*, *11*(1), 121–127. https://doi.org/https://doi.org/10.1002/aic.690110125

Ritter, J. A., Bhadra, S. J., & Ebner, A. D. (2011). On the Use of the Dual-Process Langmuir Model for Correlating Unary Equilibria and Predicting Mixed-Gas Adsorption Equilibria. *Langmuir*, *27*(8), 4700–4712. https://doi.org/10.1021/la104965w

Ross, S., & Olivier, J. P. (1961). ON PHYSICAL ADSORPTION. XII. THE ADSORPTION ISOTHERM AND THE ADSORPTIVE ENERGY DISTRIBUTION OF SOLIDS1. *The Journal of Physical Chemistry*, *65*(4), 608–615. https://doi.org/10.1021/j100822a005

Rudziński, W., & Jaroniec, M. (1974). Adsorption on heterogeneous surfaces: A new method for evaluating the energy distribution function. *Surface Science*, *42*(2), 552–564. https://doi.org/https://doi.org/10.1016/0039-6028(74)90038-7

Sanchez Varretti, F. O., Bulnes, F. M., & Ramirez-Pastor, A. J. (2016). A cluster-exact approximation study of the adsorption of binary mixtures on heterogeneous surfaces. *Applied Surface Science*, *387*, 268–273. https://doi.org/https://doi.org/10.1016/j.apsusc.2016.06.112

Sircar, S. (1987). The role of adsorbent heterogeneity in adsorption from binary liquid mixtures. *Langmuir*, *3*(3), 369–372. https://doi.org/10.1021/la00075a016

Talu, O., & Zwiebel, I. (1986). Multicomponent adsorption equilibria of nonideal mixtures. *AIChE Journal*, *32*(8), 1263–1276. https://doi.org/10.1002/aic.690320805

Valenzuela, D. P., Myers, A. L., Talu, O., & Zwiebel, I. (1988). Adsorption of gas mixtures: Effect of energetic heterogeneity. *AIChE Journal*, *34*(3), 397–402. https://doi.org/10.1002/aic.690340306

Yang, R. T. (1997). Gas Separation by Adsorption Processes. In *Series on Chemical Engineering: Vol. Volume 1*. PUBLISHED BY IMPERIAL COLLEGE PRESS AND DISTRIBUTED BY WORLD SCIENTIFIC PUBLISHING CO. https://doi.org/doi:10.1142/p037

APPENDIX A

DUAL-PROCESS LANGMUIR MODEL PARAMETERS

Table A.1 Dual-Process Langmuir (DPL) Model Parameters and Average Relative Errors (AREs) for Single-Components Adsorbates-Adsorbent Systems on H-modernite (Ritter et al., 2011).

Species	$b_{0,1}$ (kPa^{-1})	$b_{0,2}$ (kPa^{-1})	E_1 (kJ/mol)	E_2 (kJ/mol)	n^s_1 (mol/kg)	n^s_2 (mol/kg)	ARE (%)
CO_2	1.63×10^{-9}	1.44×10^{-7}	48.56	28.27	1.01	2.34	6.18
H_2S	1.10×10^{-6}	1.76×10^{-7}	38.56	33.28	1.21	1.50	2.76
C_3H_8	6.42×10^{-7}	4.92×10^{-8}	37.04	31.83	0.74	0.63	1.32

APPENDIX B

PRINCIPLE OF VIABILITY

Table B.1 Viable and Nonviable Perfect Positive (PP) and Perfect Negative (PN) correlations for a Ternary System (Ritter et al., 2011).

	Site-matching correlation							
Binary Pair	C-1	C-2	C-3	C-4	C-5	C-6	C-7	C-8
A - B	PP	PN	PP	PP	PN	PN	PP	PN
A - C	PP	PP	PN	PP	PN	PP	PN	PN
C - B	PP	PP	PP	PN	PP	PN	PN	PN
Viability	yes	no	no	no	yes	yes	yes	no